

## An experimental study of pool entrainment with side exit



Peng Zhang<sup>a,\*</sup>, Wei Li<sup>a</sup>, Zhi Di<sup>a</sup>, Xiao Hu<sup>a</sup>, Lian Chen<sup>a</sup>, Huajian Chang<sup>a,b</sup>, Peipei Chen<sup>c</sup>

<sup>a</sup>State Nuclear Power Technology R&D Center, Future SST City, Changping, Beijing, China

<sup>b</sup>Tsinghua University, Tsinghua Yuan #1, Haidian, Beijing, China

<sup>c</sup>State Power Investment Overseas Co. Ltd., North Road of 3<sup>rd</sup> Circle, Beijing, China

### ARTICLE INFO

#### Article history:

Received 2 March 2017

Received in revised form 23 June 2017

Accepted 25 June 2017

#### Keywords:

Pool entrainment  
Small break LOCA  
Thermo-hydraulic  
Reactor safety

### ABSTRACT

Pool entrainment in upper plenum is an important safety related phenomenon in SBLOCA transient for advanced PWR plants like AP1000. Due to the unique geometric characteristics, the application of standard Kataoka model in the upper plenum/hotleg entrainment phenomena requires significant caution. Based on a careful review of recent pool entrainment studies, this research carried out an experimental study of air–water pool entrainment with and without side exit/outlet to better capture the prototypic geometry of upper plenum/hotleg arrangement. Total 150 sets of test data are obtained at various combinations of gas velocities and water levels. The test data covers several entrainment regions from low gas flux region to near saturation region. The results show that the side exit/outlet will reduce the entrainment rate in high gas flux region and near saturation region. The mechanism is analyzed using visualization and CFD simulation. Based on the experiment data, a new correlation of pool entrainment with side exit/outlet in high gas flux region is proposed.

© 2017 Elsevier Ltd. All rights reserved.

## 1. Introduction

Liquid entrainment from pool surface is an important phenomenon related in reactor safety. For LOCA transient of Pressurized Water Reactors (PWR), the pool entrainment in reactor vessel's upper plenum may affect the loss of coolant process (Design Control Document, 0000; Wu et al., 2005; Xiang et al., 2016). In the postulated severe accident, the entrained liquid jet or droplet may cause the radioactive particle to leave the pool and transport to containment and environment (Cosandey et al., 2003). The most referenced pool entrainment model is developed by Kataoka and Ishii (1983), Kataoka proposed three regions in pool entrainment mechanism and modeled them differently: (a) near surface region, (b) momentum controlled region (with three sub-regimes according to gas velocity: low, intermedia and high), and (c) deposition controlled region. For each region, the statistical total entrainment rate  $E_{fg}$  (defined as the ratio of entrained liquid mass flow rate  $\rho_l j_l$  to gas mass flow rate  $\rho_g j_g$ ) is characterized as a function of gas superficial velocity  $j_g$ , two phase mixture level  $h$ , vessel diameter  $D_H$  and fluid properties. Garner et al. (1954)

and Golub (1970)'s data are used to determine the coefficients of their correlations. However, due to lack of valid test data, the correlation for high gas flux sub-regime in momentum controlled region was not determined.

The authors' previous work reported experiment results in high gas flux momentum control region and proposed a new correlation (Zhang et al., 2016). Nevertheless, as shown in Fig. 1, the existing standard pool entrainment models do not agree well with some recent reported experiment data with unique exit/outlet geometries (summarized in Table 1). The entrainment data in Fig. 1 show a significant inconsistency and evident dependence on geometries. Some literatures attribute this geometry sensitivity to 'gas acceleration near exit area', but with limited analysis.

In order to provide a better understanding of geometry effects on pool entrainment phenomena, this paper is to report an experimental study of pool entrainment at momentum controlled regime with and w/o side exit/outlet, and the influence of side exit/outlet is discussed and analyzed.

## 2. Experiment apparatus and instrumentation

The 3D schematic diagram of the experiment facility is shown in Fig. 2. An air blower is used to supply air, and the water is supplied from a water tank by gravity. The test section is made by a transparent PMMA tube with 2.2 m high and 0.38 m in diameter (D). Air and water are well mixed in a mixer before entering the

\* Corresponding author.

E-mail addresses: [zhangpeng5@snptc.com.cn](mailto:zhangpeng5@snptc.com.cn) (P. Zhang), [liwei5@snptc.com.cn](mailto:liwei5@snptc.com.cn) (W. Li), [dizhi@snptc.com.cn](mailto:dizhi@snptc.com.cn) (Z. Di), [huxiao@snptc.com.cn](mailto:huxiao@snptc.com.cn) (X. Hu), [chenlian@snptc.com.cn](mailto:chenlian@snptc.com.cn) (L. Chen), [changhj@tsinghua.edu.cn](mailto:changhj@tsinghua.edu.cn) (H. Chang), [chenpeipei@snptc.com.cn](mailto:chenpeipei@snptc.com.cn) (P. Chen).

**Nomenclature**

|          |                                                                                       |              |                                                                                                 |
|----------|---------------------------------------------------------------------------------------|--------------|-------------------------------------------------------------------------------------------------|
| $D_H$    | hydraulic diameter of vessel                                                          | $j_g$        | dimensionless superficial gas velocity defined as $j_g/(\sigma g \Delta \rho / \rho_g^2)^{1/4}$ |
| $D_H^*$  | dimensionless hydraulic diameter of vessel defined as $D_H/\sqrt{\sigma/g\Delta\rho}$ | $N_{\mu g}$  | gas viscosity number defined as $\mu_g/(\rho_g \sigma \sqrt{\sigma/g\Delta\rho})^{1/2}$         |
| $E_{fg}$ | entrainment defined as $\rho_f j_f / \rho_g j_g$                                      | $\Delta\rho$ | density difference between gas and liquid                                                       |
| $G$      | acceleration due to gravity                                                           | $\rho_f$     | density of liquid                                                                               |
| $h$      | height above the pool surface                                                         | $\rho_g$     | density of gas                                                                                  |
| $h^*$    | dimensionless height above the pool surface defined as $h/\sqrt{\sigma/g\Delta\rho}$  | $\sigma$     | surface tension                                                                                 |
| $j_f$    | superficial liquid velocity                                                           |              |                                                                                                 |
| $j_g$    | superficial gas velocity                                                              |              |                                                                                                 |

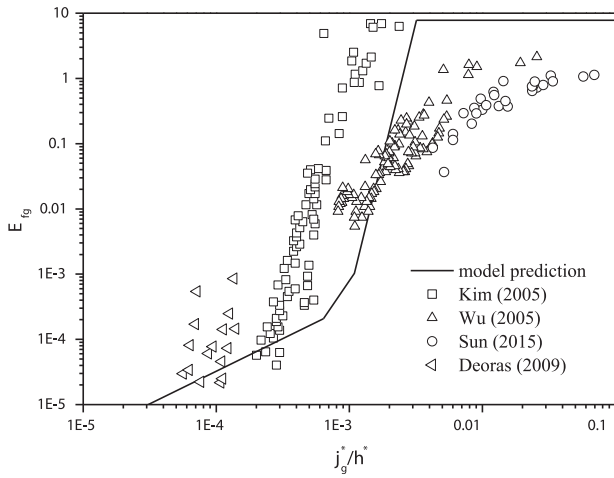


**Fig. 1.** Recent data vs. model prediction in momentum controlled and near surface region.

test section. In order to investigate the exit/outlet effects, the test section is designed in a similar arrangement to upper plenum/hot-leg in typical PWRs (as shown in Fig. 3(b)). The diameter of the side exit tube  $d$  is 50 mm, which offers a similar  $d/D$  ratio in prototypic PRW design.

$$\frac{d}{D} = 0.13; \frac{A_{exit}}{A_{test\ section}} = 0.017$$

Test data is compared with standard pool entrainment (as shown in Fig. 3(a)) data with top exit/outlet.

Pressure and temperature are measured at the inlet and outlet of the test section respectively. Temperature is measured by Type K thermocouple with uncertainty of  $\pm 1$  °C. The air flowrate is measured by two vortex flow meters with uncertainty of  $\pm 0.5\%$ . Since in the momentum controlled region, the entrainment rate changes dramatically, two entrainment measurement methods are used in this study. In large entrainment rate tests, the entrained water is separated by the moisture separator and collected in the recovery tank as shown in Fig. 2. The water is weighted by 3 load cells with an uncertainty of  $\pm 4$  kg in the recovery tank. In small entrain-

**Table 1**  
Summary of entrainment data with unique exit/outlet in recent years.

| Reference            | Fluid       | Vessel diameter (m) | Dimensionless height $h^*$ | $j_g$ (m/s) | Entrainment region                        | Type of exit |
|----------------------|-------------|---------------------|----------------------------|-------------|-------------------------------------------|--------------|
| Wu et al. (2005)     | Air-water   | 0.6                 | 0–150                      | 0.5–1.18    | Intermedia to high gas flux; near surface | Side exit    |
| Kim and No (1675)    | Air-water   | 0.3                 | 35–350                     | 0.07–0.35   | Low to high gas flux;                     | Top shrink   |
| Deoras et al. (2010) | Air-water   | 0.3                 | 125–214                    | 0.05–0.2    | Low gas flux                              | Top shrink   |
| Sun et al. (2015)    | Steam-water | 0.6                 | 0–60                       | 0.12–0.17   | High gas flux; near surface               | Side exit    |

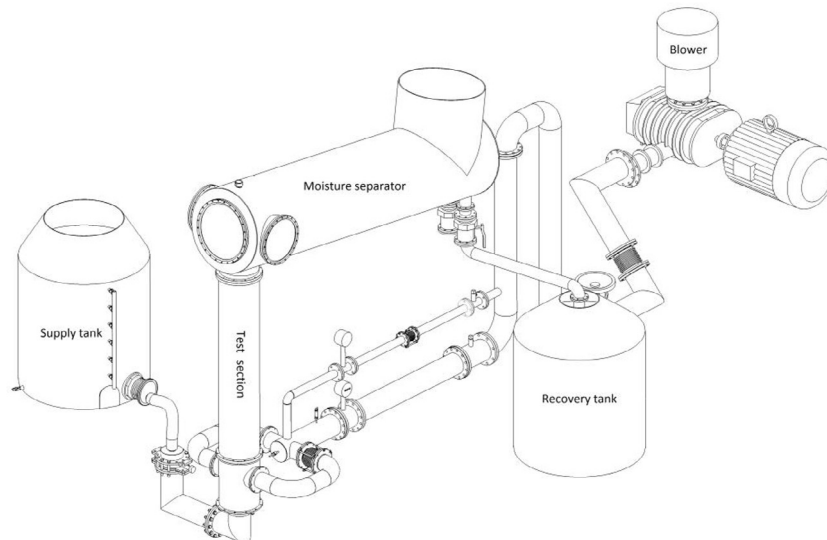


**Fig. 2.** Schematic diagram of experiment apparatus.

Download English Version:

<https://daneshyari.com/en/article/5474945>

Download Persian Version:

<https://daneshyari.com/article/5474945>

[Daneshyari.com](https://daneshyari.com)